CHEMISTRY OF MATERIALS
Article

Chem. Mater. **2009,** *21,* 4899–4904 4899
DOI:10.1021/cm9020222

Calcium Amidoborane Ammoniate—Synthesis, Structure, and Hydrogen Storage Properties

Yong Shen Chua,[‡] Guotao Wu,[†] Zhitao Xiong,[†] Teng He,[†] and Ping Chen*[,†]

[†]*Dalian Institute of Chemical Physics, Dalian 116023, People's Republic of China, and*
[‡]*Department of Chemistry, National University of Singapore, Singapore 117542, Singapore*

Received July 6, 2009. Revised Manuscript Received September 7, 2009

A new type of hydrogen storage material—namely, calcium amidoborane ammoniate ($Ca(NH_2BH_3)_2 \cdot 2NH_3$)—is synthesized by reacting calcium amide and ammonia borane in a molar ratio of 1:2. Structural analyses show that this newly developed complex has a orthorhombic structure (space group *Pna*21) with unit-cell parameters of $a = 18.673(3)$ Å, $b = 5.2283(8)$ Å, $c = 8.5748(12)$ Å, and $V = 873.16(22)$ Å^3. The presence of NH_3 in the crystal lattice facilitates the formation of dihydrogen bonding between BH···HN, which is considerably shorter than that in calcium amidoborane ($Ca(NH_2BH_3)_2$). As a consequence, the bond lengths of B−H and N−H are increased comparatively. Our experimental results show that more than 8 wt % hydrogen can be released from $Ca(NH_2BH_3)_2 \cdot 2NH_3$ without borazine emission at 150 °C.

Introduction

Compounds or complexes with high hydrogen content are potential hydrogen storage materials.[1−3] Ammonia borane (NH_3BH_3, abbreviated hereafter as AB), which is formed upon reacting alkali-metal borohydrides with ammonium salts in ether solution[4,5] and has a hydrogen capacity of 19.6 wt %, is widely regarded as one of the promising candidates for hydrogen storage. Releasing hydrogen from AB is a three-step process,[6] giving one equiv of H_2 at each step. However, releasing the last equivalent of H_2 can only be achieved at temperatures above 500 °C; thus, only the first two steps are considered for producing "usable" hydrogen. The exothermic release of 2 equiv of H_2 from AB occurs in the temperature range of 100−200 °C, because of kinetic problems.[7] To improve the dehydrogenation performance, considerable effort has been given to the chemical modification of AB. Reacting alkali-metal or alkali-earth metal hydrides with AB can produce lithium amidoborane ($LiNH_2BH_3$, or LiAB in short),[8−11] sodium amidoborane ($NaNH_2BH_3$, or NaAB in short),[8,12] and calcium amidoborane ($Ca(NH_2BH_3)_2$, or CaAB in short),[11,13,14] in which LiAB and NaAB can release ∼10.9 and ∼7.5 wt % hydrogen, respectively, at ca. 91 °C without borazine emission,[8] showing superior performance to the pristine AB. CaAB that has been synthesized via a ball-milling technique or wet-chemical process releases ∼8 wt % of hydrogen at temperatures below 250 °C.[11,13,14] Clearly, chemical compositional modification to AB which leads to the formation of many new compounds, which bring considerable changes in the dehydrogenation properties. The synthesis of amidoborane is usually via reacting alkali or alkali-earth hydrides with AB either in solution or in solid form. An alternative way is by metathesis of alkali or alkali-earth salts with AB. Xiong et al. recently reported that, when reacting $NaNH_2$ and AB in THF, $NaNH_2BH_3$ of high purity and yield can be obtained.[12] Our initial objective in this study was to synthesize high-quality CaAB (denoted as **I**) by reacting calcium amide ($Ca(NH_2)_2$) with AB in a molar ratio of 1:2, i.e., $Ca(NH_2)_2 + 2NH_3BH_3 \rightarrow Ca(NH_2BH_3)_2 + 2NH_3$. However, experimental characterizations show that NH_3 does not detach but adducts to CaAB to form a novel and high-hydrogen-content complex—namely, calcium amidoborane ammoniate ($Ca(NH_2BH_3)_2 \cdot 2NH_3$) (denoted as **II**), which has an orthorhombic structure (space group *Pna*21) identified using combined direct space simulated

*Author to whom correspondence should addressed. E-mail: pchen@dicp.ac.cn.

(1) Bogdanovic, B.; Schwickardi, M. *J. Alloys Compd.* **1997**, *253*, 1.
(2) Chen, P.; Xiong, Z.; Luo, J.; Lin, J.; Tan, K. L. *Nature* **2002**, *420*, 302.
(3) Grochala, W.; Edwards, P. P. *Chem. Rev.* **2004**, *104*, 1283.
(4) Shore, S. G.; Parry, R. W. *J. Am. Chem. Soc.* **1955**, *77*, 6084.
(5) Heldebrant, D. J.; Karkamkar, A.; Linehan, J. C.; Autrey, T. *Energy Environ. Sci.* **2008**, *1*, 156.
(6) Wolf, G.; Baumann, J.; Baitalow, F.; Hoffmann, F. P. *Thermochim. Acta* **2000**, *343*, 19.
(7) Hu, M. G.; Geanangel, R. A.; Wendlandt, W. W. *Thermochim. Acta* **1978**, *23*, 249.
(8) Xiong, Z. T.; Yong, C. K.; Wu, G. T.; Chen, P.; Shaw, W.; Karkamkar, A.; Autrey, T.; Jones, M. O.; Johnson, S. R.; Edwards, P. P.; David, W. I. F. *Nat. Mater.* **2008**, *7*, 138.
(9) Kang, X.; Fang, Z.; Kong, L.; Cheng, H.; Yao, X.; Lu, G.; Wang, P. *Adv. Mater.* **2008**, *20*, 2756.
(10) Xiong, Z. T.; Chua, Y. S.; Wu, G. T.; Xu, W. L.; Chen, P.; Shaw, W.; Karkamkar, A.; Linehan, J.; Smurthwaite, T.; Autrey, T. *Chem. Commun.* **2008**, 5595.
(11) Wu, H.; Zhou, W.; Yildirim, T. *J. Am. Chem. Soc.* **2008**, *130*, 14834.
(12) Xiong, Z. T.; Wu, G. T.; Chua, Y. S.; Hu, J. J.; He, T.; Xu, W. L.; Chen, P. *Energy Environ. Sci.* **2008**, *1*, 360.
(13) Diyabalanage, H. V. K.; Shrestha, R. P.; Semelsberger, T. A.; Scott, B. L.; Bowden, M. E.; Davis, B. L.; Burrell, A. K. *Angew. Chem., Int. Ed.* **2007**, *46*, 8995.
(14) Spielmann, J.; Jansen, G.; Bandmann, H.; Harder, S. *Angew. Chem., Int. Ed.* **2008**, *47*, 6290.

Published on Web 10/05/2009

annealing method and first-principles calculations. Thermal decomposition analyses show that, under a dynamic flow mode where gaseous product(s) can be blown away immediately from the solid reactant, **II** undergoes deammoniation at ca. 73 °C and forms **I**; however, if the thermal decomposition is conducted in a close system where the gaseous product is kept in the vicinity of the solid reactant, **II** releases hydrogen (ca. 8 wt %) rather than NH_3 in the temperature range of 70−150 °C, showing the participation of NH_3 in the H_2 production. The presence of adductive NH_3 in **II** leads to a shortened NH···HB dihydrogen bond in the structure and may facilitate low-temperature dehydrogenation.

Materials and Methods

NH_3BH_3 powder (97% purity) was purchased from Aldrich. $Ca(NH_2)_2$ was synthesized on site by reacting calcium granules (98.5% purity, Merck) with purified ammonia gas at room temperature for one day. The percentage yield of $Ca(NH_2)_2$ is 98%, which was calculated from a weight gain of ~80% ($Ca + 2NH_3 \rightarrow Ca(NH_2)_2 + H_2$). The formation of $Ca(NH_2)_2$ was further confirmed by the X-ray diffraction (XRD) and Fourier transform infrared (FTIR) characterizations. The $Ca(NH_2)_2-NH_3BH_3$ sample, in an amide to AB molar ratio of 1:2, was ball-milled on a Retsch PM400 planetary mill at 200 rpm under an inert atmosphere for 10 h. All the material handlings were performed inside a glovebox that was filled with purified argon.

Temperature-programmed desorption (TPD) and differential scanning calorimetry (DSC) were used to investigate the thermal gas desorption of the post-milled samples. Details of the operation procedure have been mentioned elsewhere.[15] In both TPD and DSC measurements, a dynamic flow mode was applied in which purified argon was used as carrier gas and the heating rate were set at 2 °C/min. The gaseous products formed in the heating process were eluted from the reacting system. Quantitative measurements of gas evolution from samples were performed on a custom-made volumetric release reactor. NH_3 concentration was determined by exposing gaseous product(s) to $MgCl_2$ anhydrous (pretreated at 500 °C under dynamic vacuum) and further measuring its weight gain. XRD data were collected using a Bruker Model D8 Advance X-ray diffractometer with Cu Kα radiation at a power of 40 kV/40 mA. Stepwise scans were performed in the 2θ range of 10°−60° at a step of 0.05°. The obtained data were indexed using the TREOR or DICVOL programs. Candidate structures were obtained by performing simulated annealing with four formula units of $Ca(NH_2BH_3)_2 \cdot 2NH_3$ in the unit cell.[8] Rietveld refinement structural analyses were performed using the Rietica program.[16] FTIR measurements were conducted on a Varian 3100 unit in DRIFT mode. ^{11}B magic-angle-spinning (MAS) solid-state NMR experiments were conducted at room temperature on a Bruker Model DRX 400 NMR spectrometer and the ^{11}B NMR signals were referenced to $BF_3 \cdot Et_2O$ at 0 ppm.

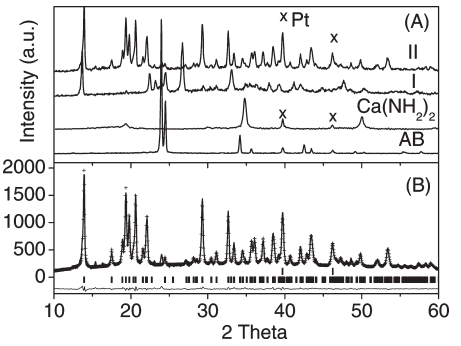

Figure 1. (A) XRD patterns of AB, $Ca(NH_2)_2$, **I** (derived by heating **II** at 100 °C under vacuum), and **II**; (B) experimental (smooth line) and calculated (+) profiles of **II**. The differences between the experimental and calculated values are shown below the observed patterns.

Theoretical Calculation. First-principles calculations based on the density functional theory (DFT) and the pseudo-potential plane wave method were performed using the Vienna ab initio simulation package (VASP).[17,18] The projector augmented wave (PAW) pseudo-potentials were used with a cut-off energy of 500 eV.[19] The generalized gradient approximation (GGA-PW91) was used to treat the electronic exchange-correlation energy. In the geometry optimization on the resulting candidate structure, full ionic relaxation and volumetric relaxation were conducted until self-consistency was achieved within a tolerance of a total energy of 0.01 meV and atomic forces of 0.01 eV/Å. The experimentally determined cell parameters were compared with the relaxed structures such that unstable candidates can be ruled out. The total energies of the relaxed structures at 0 K were also evaluated, which was used to derive the most accurate crystal structure of calcium amidoborane ammoniate (**II**).

Results and Discussion

Synthesis and Characterization of II. Negligible amount of gaseous product was detected in the sample vessel after ball-milling $Ca(NH_2)_2$ and AB in a molar ratio of 1:2 at 200 rpm for 10 h. XRD measurement on the white powdery residue collected at the end of ball milling evidenced the disappearance of starting chemicals, i.e., $Ca(NH_2)_2$ and AB (Figure 1A), and the appearance of a new set of diffraction peaks, which does not match with any known compound that contains elemental calcium, boron, nitrogen, and hydrogen, indicating the formation of **II**, according to reaction 1.

$$Ca(NH_2)_2 + 2NH_3BH_3 \rightarrow Ca(NH_2BH_3)_2 \cdot 2NH_3 \ (\mathbf{II}) \quad (1)$$

The XRD reflections can be indexed using the orthorhombic cell with lattice constants of a = 18.673(3) Å,

(15) Xiong, Z. T.; Wu, G. T.; Hu, J. J.; Chen, P. *Adv. Mater.* **2004**, *16*, 1522.
(16) Wu, G. T.; Xiong, Z. T.; Liu, Y. F.; Hu, J. J.; Chen, P.; Feng, Y. P.; Wee, A. T. S. *Inorg. Chem.* **2007**, *46*, 517.
(17) Kresse, G.; Hafner, J. *Phys. Rev. B* **1993**, *47*, 558.
(18) Kresse, G; Furthmuller, J. *Comput. Mater. Sci.* **1996**, *6*, 15.
(19) Kresse, G; Joubert, D. *Phys. Rev. B* **1999**, *59*, 1758.

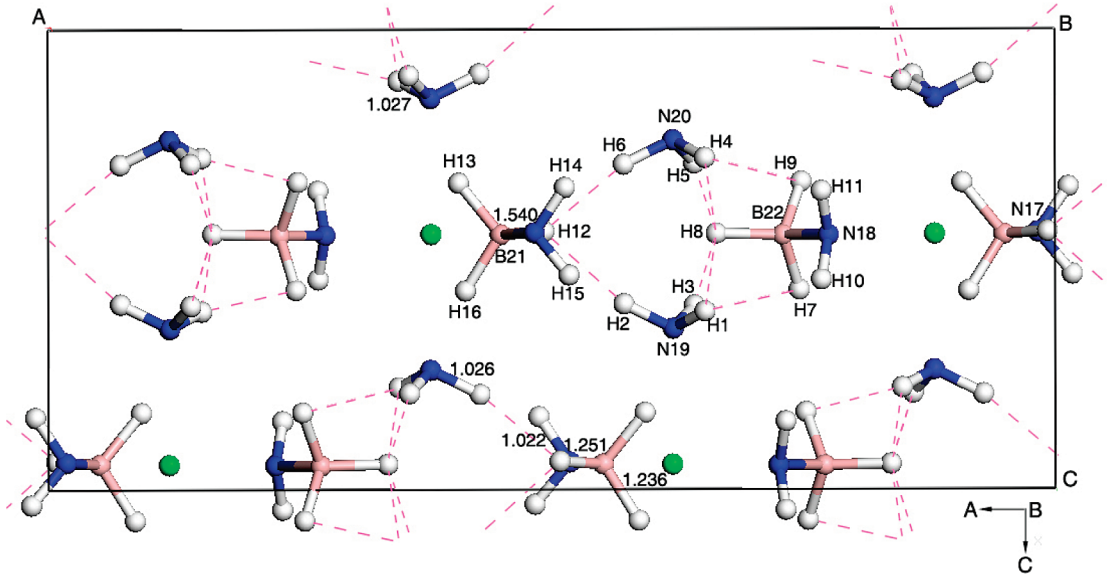

Figure 2. Molecular packing and network of N−H···H−B dihydrogen bonding in the crystal of **II**. Calcium is represented by green spheres, nitrogen by blue spheres, boron by pink spheres, and hydrogen by white spheres.

$b = 5.2283(8)$ Å, $c = 8.5748(12)$ Å, and $V = 873.16(22)$ Å^3. The space group of *Pna*21 (No. 33) was assigned based on the systematic absences. The crystal structure of this new phase was then solved using the combined direct space simulated annealing method and first-principles calculations. In the several candidate models generated from direct space simulated annealing, NH_2BH_3 and NH_3 were kept as rigid bodies with common bond lengths and bond angles. First-principles calculations were then performed to identify the most stable structure and favorable hydrogen positions. The structure obtained from first-principles calculations has lattice constants of $a = 18.6301$ Å, $b = 5.2913$ Å, $c = 8.5016$ Å, which is consistent with the indexing result. Because the number of reflections in the powder XRD pattern is inadequate to allow independent determination of atomic fractional coordinates, atomic fractional coordinates from first-principles calculations were used in the Rietveld structural refinements. The Rietveld fit shown in Figure 1B is in excellent agreement with the experimental powder XRD pattern, yielding the agreement factors of $R_p = 9\%$ and $R_{wp} = 12\%$. The detailed structural information is given in the Supporting Information.

The fully relaxed structure from first-principles calculations is shown in Figure 2. Constitutional molecules are present in planes parallel to the *ab* plane. Each Ca cation is sandwiched between two NH_3 ligands along the *c*-axis. Therefore, an ammoniate of calcium amidoborane with the chemical formula of $Ca(NH_2BH_3)_2 \cdot 2NH_3$ (**II**) was formed upon reacting $Ca(NH_2)_2$ and 2 equiv of AB, according to reaction 1. The $-NH_2$ group in $Ca(NH_2)_2$ is a stronger base than NH_3, because of the poorer electron negativity of the Ca atom compared to the H atom; therefore, $-NH_2$ is likely to abstract BH_3 from NH_3 in AB and establish a stronger dative bond. The other possibility is that $-NH_2$ abstracts one H atom from NH_3 in AB and creates NH_3 and $-NH_2BH_3$. The

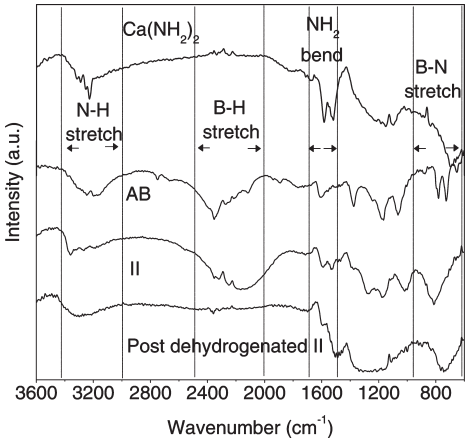

Figure 3. FTIR spectra of $Ca(NH_2)_2$, AB, **II**, and the post-dehydrogenated **II** sample.

generated NH_3, on the other hand, adducts to the newly formed $Ca(NH_2BH_3)_2$ or **I** and forms **II**. The B−N bond lengths in **II** are in between 1.540 and 1.553 Å, shorter than that in AB (~1.58 Å), which reveals a stronger bonding between B and N, agreeing well with the IR and NMR observations (see Figure 3 and 4). It is worthy of mentioning that the B−H bond in **II** is longer than that in AB, which is the consequence of strengthened B−N dative bonding and the existence of dihydrogen bond between $-BH_3$ and the coordinated NH_3. The N−H bond length in the coordinated NH_3 (1.026−1.027 Å) also increases, compared with the N−H bonds (1.020 Å) in NH_3 gas, which are likely due to two main factors, i.e., (1) the N atom in NH_3 (Lewis base) donates its lone pair to the Ca cation (Lewis acid), and (2) the presence of dihydrogen bonding between the NH_3 and the adjacent BH_3 in $[NH_2BH_3]^-$. As shown in Figure 2 and Table 1, the calculated shortest BH···HN intermolecular distance (H−H distance) is 1.927 Å, which is significantly shorter than the van der Waals distance. The ∠NH···H in **II**,

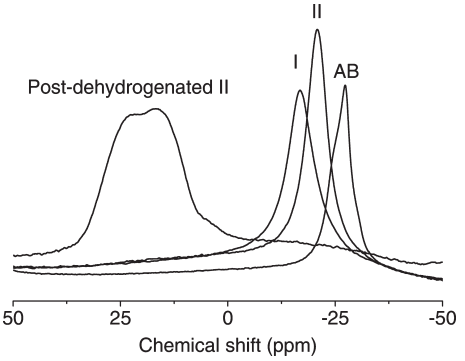

Figure 4. ^{11}B MAS solid-state NMR spectra of AB, **I**, **II**, and the post-dehydrogenated **II** sample.

Table 1. Interatomic Distances and Bond Angles for Dihydrogen Bonds in II

interatomic distance	(Å)	bond angle	(°)	bond angle	(°)
H1···H7	2.087	B21−H12···H2	119.3	N19−H1···H7	158.4
H1···H8	2.358	B21−H12···H6	124.2	N19−H1···H8	146.9
H2···H12	1.997	B22−H7···H1	102.9	N19−H2···H12	163.8
H3···H8	2.274	B22−H8···H3	104.4	N19−H3···H8	164.7
H4···H8	2.344	B22−H8···H5	106.0	N20−H4···H8	147.4
H4···H9	2.118	B22−H8···H4	91.1	N20−H4···H9	157.6
H5···H8	2.265	B22−H8···H1	89.6	N20−H5···H8	165.4
H6···H12	1.927	B22−H9···H4	102.2	N20−H6···H12	165.3

which are in the range of 150−170°, are consistent with those found in AB. The ∠BH···H, on the other hand, become more twisted in the range of 85−125°, compared to that of AB (95−115°).[20] A network is established throughout the entire volume of the cell in which the dihydrogen bonds link individual $[NH_2BH_3]^-$ in a Ca$(NH_2BH_3)_2$ layer parallel to the *ab* plane, leading to a special arrangement of Ca coordination in the crystal (i.e., Ca is not of perfect octahedral coordination, because of the existence of dihydrogen bonding, which is different from the Ca$(NH_2BH_3)_2\cdot$2THF crystal, where intermolecular interactions between the Ca cation and hydridic hydrogen in $[NH_2BH_3]^-$ result in an extended chain structure in which Ca seating in the octahedral center coordinates with two NH_2 groups, two BH_3 groups, and two THF molecules).[13,14]

FTIR characterization on **II** revealed that neither the characteristic N−H symmetric and asymmetric stretches of Ca$(NH_2)_2$ at 3316, 3290, 3255, and 3228 cm^{-1}[21] nor the NH_2 bending at 1585 and 1524 cm^{-1} were detectable (see Figure 3). However, the B−H (in the range of 2150−2270 cm^{-1}) and B−N stretches (ca. 800 cm^{-1}) show a red shift and a blue shift, compared to AB,[22,23] indicating a weakened B−H bond and strengthened B−N bond, respectively, which agree well with the changes in bond lengths previously mentioned. A single boron species resonating

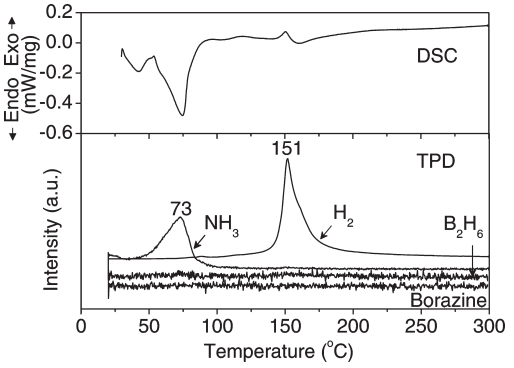

Figure 5. DSC and TPD measurements on the decomposition of **II**.

at −21 ppm was observed by magic-angle spinning (MAS) solid-state ^{11}B NMR (shown in Figure 4), which has a 6 ppm downfield shift, compared to that of pristine AB (−27 ppm), showing that the B atom received more electrons from the N atom, which is consistent with the enhanced B−N bond observed in FTIR spectroscopy.

Deammoniation of II. As pictured in the structural model (Figure 2), the Ca center is coordinated with two NH_3 molecules. The adduct nature of NH_3 in this newly formed complex is further evidenced by the temperature-programmed desorption (TPD) characterization. As shown in Figure 5, the decomposition of **II** occurs right above room temperature and reaches a maximum rate at ∼73 °C; the decomposed gaseous product is mainly ammonia at temperatures below 100 °C, a temperature that is much lower than that of the self-decomposition of Ca$(NH_2)_2$.[21] Noted that borazine and diborane were undetectable by mass spectrometry. A weight loss of ∼25.3 wt % was detected by holding the sample at 100 °C under a flow of purified argon, which is equivalent to ∼2 mol of NH_3. Also evidenced from the DSC measurement is the fact that the NH_3 liberation is a mild endothermic process, indicating the NH_3 release and absorption is reversible (see Figure 5). Indeed, by exposing the deammoniated sample (0.15 g) under a NH_3 pressure of 4 psi at ambient temperature overnight, **II** can be regenerated (as evidenced by the XRD characterization shown in Figure S1 of the Supporting Information). XRD measurement of the deammoniated sample gave a pattern identical to **I** reported by Wu et al.[11] (monoclinic space group *C*2, with lattice constants of a = 9.1000 Å, b = 4.3710 Å, c = 6.4110 Å, and β = 93.1900°). Therefore, the decomposition of **II** under dynamic flow can be described in reaction 2:

$$\text{Ca}(\text{NH}_2\text{BH}_3)_2\cdot 2\text{NH}_3\ (\mathbf{II}) = \text{Ca}(\text{NH}_2\text{BH}_3)_2\ (\mathbf{I}) + 2\text{NH}_3 \quad (2)$$

Compared to complex **II**, the Ca atom in **I** satisfies its octahedral coordination by direct bonding with two N atoms from $[NH_2BH_3]^-$ and four $-BH_3$ groups from other $[NH_2BH_3]^-$. Although the Ca−N bond distance in **I** (∼2.466 Å)[11] is similar to those in **II** (2.397−2.521 Å), the Ca−B bond distances of **I** (2.87−3.03 Å)[11] were considerably longer than those in **II** (2.650−2.807 Å), which lead

(20) Klooster, W. T.; Koetzle, T. F.; Siegbahn, P. E. M.; Richardson, T. B.; Crabtree, R. H. *J. Am. Chem. Soc.* **1999**, *121*, 6337.
(21) Xiong, Z. T.; Wu, G. T.; Hu, J. J.; Chen, P. *J. Alloys Compd.* **2007**, *441*, 152.
(22) Sepehri, S.; Feaver, A.; Shaw, W. J.; Howard, C. J.; Zhang, Q.; Autrey, T.; Cao, G. *J. Phys. Chem. B.* **2007**, *111*, 14285.
(23) Hess, N. J.; Bowden, M. E.; Parvanov, V. M.; Mundy, C.; Kathmann, S. M.; Schenter, G. K.; Autrey, T. *J. Chem. Phys.* **2008**, *128*, 034508.

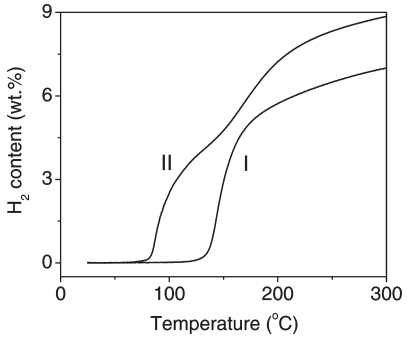

Figure 6. Volumetric release of **I** and **II**; the temperature was increased to 300 °C at a ramping rate of 0.5 °C/min.

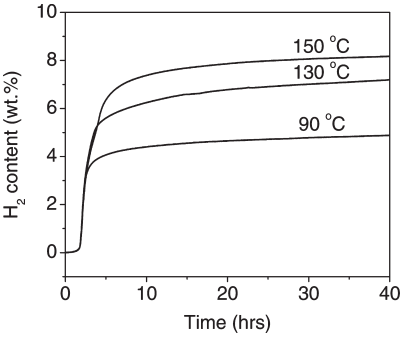

Figure 7. Volumetric release of **II** at preset temperatures. Samples were heated to the present temperature at a ramping rate of 0.5 °C/min.

to a downfield shift of 4 ppm, compared to that for **II** in ^{11}B MAS NMR characterization (see Figure 4), showing that the B atom is deshielded after deammoniation. The process shown in reaction 2 can be applied as an alternative way to prepare **I**, which was synthesized previously by reacting CaH_2 with AB in THF, where THF is difficult to be removed completely, because of a strong adductive effect.[13]

The second-step dehydrogenation of **II** at temperatures above 120 °C (shown in Figure 5) is due to the thermal decomposition of **I**.

Dehydrogenation of II. As shown in Figure 5, the decomposition of **II** under the dynamic flow mode (i.e., TPD) is a two-step process that evolves 2 equiv of NH_3 below 100 °C and hydrogen at temperatures above 120 °C. However, when conducting volumetric release measurement in a closed system, where gaseous products were kept in the vicinity of the solid reactant, different features were observed. As shown in Figure 6, little pressure increase was detected at temperatures below 70 °C, showing the relatively low equilibrium pressure of NH_3 in the **II** system. In other words, the majority of NH_3 should remain in the lattice of **II**. When temperature was increased above 70 °C, a relative rapid pressure increase was observed. After keeping the sample at 80 °C for 2 h, a pressure increase of 44.5 psi was observed (see Figure S2 in the Supporting Information). Mass spectrometry analysis of the gaseous products in the reactor evidenced that the majority of gas was H_2 (see Figure S3 in the Supporting Information). Clearly, the pathway of thermal decomposition of **II** changes with the conditions that are applied (closed system or dynamic flow); in this sense, we believe that the presence of NH_3 plays an essential role. Under the dynamic flow mode (i.e., TPD conditions), the instant pressure of NH_3 around the solid reactant is almost zero, because NH_3 that had detached from **II** was blown away immediately by the carrier gas (argon). However, in a close system, NH_3, which remains in the vicinity of the reactant either within the lattice of **II** or in the intimate gaseous phase, creates an option to interact with species nearby (either within the lattice of **II** or through gas−solid interaction). As a consequence, N−H in NH_3 dissociates, the N atom is retained in the solid phase and H moves to the gas phase as H_2. The profile of dehydrogenation of **I** in the closed

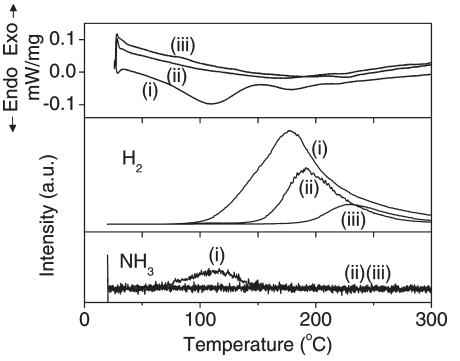

Figure 8. DSC and TPD measurements on the **II** samples collected after volumetric release at (i) 90, (ii) 130, and (iii) 150 °C.

system is also shown in Figure 6. The reduced dehydrogenation temperature for **II**, compared with **I**, may partially be due to the stronger dihydrogen bonding and the weakened B−H bond in **II**. An amount of H_2 (5.9 equiv., or 8.8 wt %) was released from **II** upon heating to 300 °C. Quantitative measurement on NH_3 residue in the gaseous phase was done by conducting the accumulated desorption gas into a flask that contained anhydrous $MgCl_2$. Anhydrous $MgCl_2$ was used, because of its relatively low equilibrium ammonia pressure (1.5×10^{-6} bar) at 80 °C when forming ammoniate ($MgCl_2 \cdot NH_3$).[24,25] Calculated from the weight gain of $MgCl_2$, NH_3 that had survived in the gas phase is <0.1 equiv. To determine whether the heating rate has an effect on the decomposition of **II**, we tested the decomposition **II** in the closed system to 150 °C at heating rates of 0.5, 2, and 5 °C/min, respectively. As shown in Figures S4, S5, S6, and S7 in the Supporting Information, the gaseous product was H_2 in all cases at the end of the volumetric measurement.

Because ca. 5.9 equiv H_2 was released from the sample, the overall dehydrogenation can be described by reaction 3:

$$Ca(NH_2BH_3)_2 \cdot 2NH_3 \rightarrow [CaB_2N_4H_4] + 6H_2 \qquad (3)$$

Our preliminary attempt of rehydrogenating the white amorphous powder $[CaB_2N_4H_4]$ under a H_2 pressure of 50 bar in the temperature range of 20−300 °C was

(24) Lepinasse, E.; Spinner, B. *Int. J. Refrig.* **1994**, *17*, 309.
(25) Christensen, C. H.; Sorensen, R. Z.; Johannessen, T.; Quaade, U. J.; Honkala, K.; Elmoe, T. D.; Kohler, R.; Norskov, J. K. *J. Mater. Chem.* **2005**, *15*, 4106.

unsuccessful. The ^{11}B MAS NMR spectrum of $[CaB_2N_4H_4]$ presents a broad lineshape with two overlapping ^{11}B peaks, at 15.7 and 24.9 ppm (see Figure 4), which is due to the second-order quadrupolar interaction. A similar lineshape was observed in the study of hexagonal BN[26,27] and $Ca_3(BN_2)_2$.[28] The B species in $[CaB_2N_4H_4]$ is likely in a BN_3 or BN_2 environment. From a stoichiometric point of view, $[CaB_2N_4H_4]$ could be a mixture of $Ca(NH_2)_2 + 2BN$ or a ternary imide of $CaB_2(NH)_4$. $Ca(NH_2)_2$ decomposes to CaNH and NH_3 readily at 150 °C; thus, it is unlikely to survive under the present reaction conditions (heated up to 300 °C). The imide form is of greater possibility. FTIR characterization clearly shows the presence of a broad imide-like N−H stretch in the region of 3100−3400 cm^{-1} (see Figure 3). B−H stretches, on the other hand, disappeared after dehydrogenation, which agrees well with the NMR observation of the BN_3 or BN_2 environment.

To shine a light on the thermodynamic and kinetic properties of dehydrogenation of this newly developed complex, **II** underwent volumetric release at 90, 130, and 150 °C, respectively. As shown in Figure 7, ca. 4.7, 7.1, and 8.2 wt % of H_2 can be released, respectively, in which more than 80% of the hydrogen can be released within 2 h. In other words, ca. 4.1. 1.7, and 0.6 wt % of hydrogen remained in those samples, respectively. XRD characterization shows that no structural information can be obtained from all three samples, because of the amorphous phases in nature. The DSC and TPD results on those samples (Figure 8) show that, except for a relatively intense endothermic peak at ca. 100 °C, which is due the removal of NH_3 from the sample, the desorption of the remaining hydrogen in all three samples exhibit mild endothermic nature, which is clearly different from the exothermic behavior observed in ammonia borane[6] and alkali-metal amidoborane,[8] an encouraging thermodynamic improvement for the amidoborane system. It is also reasonable to assign the slower dehydrogenation at lower temperature to the presence of kinetic barriers rather than thermodynamic constraint, where catalytic modification is needed to further optimize calcium amidoborane ammoniate for hydrogen storage.

(26) Jeschke, G.; Hoffbauer, W.; Jansen, M. *Solid State Nucl. Magn. Reson*. **1998**, *12*, 1.
(27) Marchetti, P. S.; Kwon, D. K.; Schmidt, W. R.; Interrante, L. V.; Maciel, G. E. *Chem. Mater*. **1991**, *3*, 482.
(28) Worle, M.; Altenschildesche, H. M.; Nesper, R. *J. Alloys Compd.* **1998**, *264*, 107.

Conclusion

A new type of hydrogen storage material—i.e., calcium amidoborane ammoniate (**II**)—has been synthesized by reacting $Ca(NH_2)_2$ and ammonia borane (NH_3BH_3, abbreviated as AB) in a molar ratio of 1:2. **II** was identified to crystallize in the orthorhombic space group *Pna*21. The cell parameters and atomic fractional coordinates were refined by the Rietveld methods. This newly developed ammoniate decomposes to hydrogen, beginning at ca. 70 °C, and can release ~5.5 equiv of H_2 (8.2 wt %) upon heating at 150 °C.

Acknowledgment. The authors thank the 863 (2009AA05Z108) and Hundred Talent Projects (KGCX2-YW-806 & KJCX2-YW-H21) and the scholarship from the National University of Singapore. The authors also appreciate beneficial discussions with Thomas Autrey and other collaborators under the IPHE project "Combination of Amine Boranes with MgH_2 & $LiNH_2$ for High Capacity Reversible Hydrogen Storage".

Supporting Information Available: Tables of calculated structural parameter, bond lengths and angles for **II**. Volumetric release of **II** at 80 °C and MS signals of the gaseous product formed after heating. Volumetric release of **II** to 150 °C at heating rates of 0.5, 2, and 5 °C/min and MS signals of the gaseous products formed after heating. This material is available free of charge via the Internet at http://pubs.acs.org.